Available online at www.sciencedirect.com

SciVerse ScienceDirect

Procedia Engineering 52 (2013) 548 – 556

Procedia Engineering

www.elsevier.com/locate/procedia

Experimental Study of N-Heptane Pool Fire Behaviors under Dynamic Pressures in an Altitude Chamber

Jiusheng Yin[a], Wei Yao[a], Quanyi Liu[a], Nan Wu[a] , Zhihui Zhou[b], Yi Wu[c], Hui Zhang[a,*]

[a]*Institute of Public Safety Research, Tsinghua University, Beijing 100084, China*
[b]*State Key Laboratory of Fire Science, University of Sci.& Tech. of China, Hefei 230027, China*
[c]*Civil Aviation Flight University of China, Guanghan 618307, .China*

Abstract

The experimental observation of pool fires under dynamic pressure is of significant meaning to understand the fire behaviors under different low pressure environments. Previous studies on low-pressure fires mainly focused on fire behaviors at static low pressure, where the fire tests were usually conducted at several discrete altitudes. An altitude chamber of size 3 m× 2 m× 2 m has been built for this study, where different dynamic pressure descent rates were configured to simulate pool fire behaviors under different low pressures. In each test, the chamber pressure varies from standard atmospheric pressure 101.3 KPa to 34 KPa. The dynamic pressure descent rate is controlled by replenishing air at different rates: 0, 15 and 20 Nm3/h. The study tested two different sizes of pool fires, where the pan heights are all 2 cm and the pan diameters are 6 cm and 10 cm respectively. N-Heptane with industrial purity of 99% was used as the testing fuel. Parameters were measured along the whole burning process, including axial flame temperature, burning rate, radiative heat flux, chamber pressure as well as fire video recording. Some specific phenomena were observed for the fires under dynamic depressurization, e.g. the flame transmitted from turbulent to laminar and its base turned blue as pressure drops, then in the final burning stage a polyhedral flame appeared and swirled in the pan until extinguishment. The measurement data, i.e. mass burning rate, flame temperature and radiative heat flux, were analyzed to reveal the pressure effect in influencing fire behaviors.

Selection and peer-review under responsibility of School of Engineering of Sun Yat-sen University

Keywords: low pressure; altitude chamber; N-Heptane; pool fire; fire behavior

1. Introduction

Tibet plateau, also called *Roof of the World*, is the highest region on Earth, with an average altitude of 4,500 m. Tibet plateau north of the Himalayas is a mysterious, exotic place for many visitors. Tibet plateau has an area of about 2.5 million square kilometers, about 25% the size of China. In recent year, the huge national investments in public transportation of Tibet allow more outsiders to get access to the once isolated plateau. Tibet railway was opened in 2006 and till now 7 airports such as Lhasa Gongga airport (altitude 3600 m) and Bangda airport (altitude 4334 m) in Tibet have been opened with more under construction. With the rapid growth of economic and social activities in Tibet, more and more people are attracted to travel, trade and live in Tibet. Tibet has over 1000 ancient buildings, numerous places of interests and unique religious culture, which are expected to attract over 12 million tourists in 2012. Tibet has unique natural ecological environment, which contains over 50% of rare wild animals of the country. The ecological environment of Tibet plateau is weak and therefore n*eeds to be protected from external activities, especially hazardous fires. The research on the high altitude fire behaviors is important to protect those valuable ancient buildings, natural sceneries, religious culture and folk residences.

One of the marked characteristics of high-altitude plateau environment is low pressure and low oxygen concentration, under which fire behaviors are apparently different with those under standard atmospheric pressure, e.g., low burning rate

* Corresponding author. Tel.: +86-10-62792861; fax: +86-10-62792683.
E-mail address: zhhui@tsinghua.edu.cn

Selection and peer-review under responsibility of School of Engineering of Sun Yat-sen University
doi:10.1016/j.proeng.2013.02.184

and radiative heat flux, but higher flame temperature and flame height. Previous fire tests at different static pressures have preliminarily shown the impact of low pressure on fire behaviors. Wieser et al [1] transported a mobile test platform by a helicopter to test EN54 fires at 4 altitudes from 400 m (97 Kpa) to 3000 m (71 KPa), where the test results demonstrated that the burning rate decreased with pressure P for about $\sim P^{1.3}$. Li et al [2] and Hu et al [3] have comparatively testes N-Heptane pool fires and wood crib fires in two cities of different altitudes. The tests [2, 3] showed that the burning rate at higher altitude is lower for about $\sim P^{1\text{-}1.3}$, so is the flame radiation; but the flame temperature is slightly higher at higher altitude and the soot volume fraction decreases with pressure as $\sim P^{0.9}$. In the tests of Li and Hu et al [2, 3], it is observed that the flame shape changed under low pressure, i.e. the flame is prolonged in height but thinner in diameter. Fang et al [4] tested different sizes of N-Heptane pool fires and confirmed that the burning rate is in linear proportion to pressure, but the pulsation frequency of flame and the CO concentration increases at higher altitudes. Ris et al [5, 6] showed that the burning rate of fuel can be scaled with pressure by $\sim P$. The fire tests of different fuels, Jet-A fuel, propanol and acrylic, in a small-scale altitude chamber by Hill [7] have shown that the burning rates decrease approximately linearly with the equivalent altitude.

It can be seen that the fire prevention and suppression at high altitude will be considerably different from that at sea level because of the special fire behaviors under low pressure. Currently, the methods and techniques to prevent and suppress fires in Tibet plateau is as the same as those adopted in sea-level cities. For this reason, fire safety research for low-pressure environments is urgent to improve the fire safety status of ancient buildings, airports and folk residences in high altitude regions. The fundamental theory and engineering practice of firefighting in high-altitude plateaus should be established of the first priority for high-altitude fire safety, which then provides foundation work for the formulation of fire protection regulation in high altitude regions.

Understanding of fire behaviors under low pressure is the first step towards establishing fire protection engineering for high-altitude plateaus. To facilitate altitude fire tests, a high-altitude fire lab has been built in Lhasa, the capital city of Tibet. Building of fire labs at other altitudes in Tibet is not ready because the lab facility is not available yet. Conducting fire tests at high-altitude plateaus is costly in expense and experimental period, because of the long-distance shipment of experimental equipment and materials to Tibet. Constrained by experimental condition and cost, high-altitude fire test data were still scarce.

Fire tests under dynamic pressure were useful to observe the continuous variation of fire behaviors during depressurization, however, limited by experimental condition few such studies were reported in the literature. Previous altitude fire tests were all conducted under a limited number of static pressure environments, such as at Hefei (Sea-level city), Lhasa (altitude 3650 m) and Dongxiong (another Tibet city with altitude 4200 m) [2, 3, 8]. In static pressure fire studies, the general trends of fire behaviors were concluded from the fitting of discrete pressure data. The observation of fire behaviors under dynamic pressure variation can systematically reveal their dependence on pressure, i.e. the dependence of mass burning rate, radiative heat flux and flame temperature on pressure.

In order to observe the continuous variation of fire behaviors during depressurization, an altitude chamber was built to simulate high altitude environments. Two different sizes of N-Heptane pool fires were tested in the altitude chamber, where the dynamic pressure drops from 101.3 KPa to 34 KPa at different descent rates. Mass burning rate, flame temperature and radiative heat flux were measured, then corresponding analysis were conducted to theoretically describe the pressure effect. The study is of significant meaning for fire safety design and fire regulation formulation in high-altitude regions.

2. Experimental design and measurements

The effective internal size of the low pressure chamber used in the experiment is 3 m× 2 m× 2 m as showed in Fig. 1. Based on the structure strength and the sealing performance of the chamber, the working pressure designed for the chamber is between 26.4 KPa -101.3 KPa, which is equivalent to the altitudes from sea level (0 m) to 10,000 m. The pressure of the low pressure chamber can be adjusted and controlled through the manipulation of the pumping rate of the vacuum pump from the control platform. The dynamic pressure range for fire tests is between 101.3 KPa and 34 KPa in this study, but at different descent rates. In the experiment, the vacuum pump will operate and pump out the air from the low pressure chamber at a fixed volume rate, to make the pressure inside the chamber decrease at a constant rate. Although the pumping rate of the vacuum pump was fixed, the pressure descent rates were adjusted by replenishing air at different rates. Three different air supplying rates, i.e. 0, 15 and 20 Nm^3, were configured to produce different descent rates of chamber pressure.

Table 1 summarizes the main experimental configurations of the chamber pool fire tests. The experimental setup of N-heptane pool fire tests is shown as Fig 2. As restricted by the volume of the low pressure chamber and the oxygen content available in the chamber, the maximum size of pool fires can be contained is 10 cm. In this study, two small round pans were used, where the diameters are 6 cm and 10 cm respectively, and the heights are all 2 cm. The testing fuel is N-Heptane with industrial purity above 99% (the impurity contents: volatile ≤ 0.05%, water ≤ 0.05%, unsaturated compounds in Br^+ ≤

0.032%), whose density is 83 ~ 685 kg/m3, boiling range is 96.5-98.5 ℃, self-ignition temperature is 223.0 ℃ and the explosion limits is 1.05–6.7%. The 6-cm-diameter pan was initially filled with 28 g liquid N-Heptane, while the 10-cm-diameter pan was filled with 80 g fuel. The measured parameters include axial flame temperature, mass burning rate, radiative heat flux, chamber pressure and fire video recording.

The instrument layout is shown as Fig 3. An array of 14 K-Type Nickel Cadmium thermocouples labeled as T1-T14 from the bottom up to the top was laid on the centerline above the pan to measure the flame temperature. T1-T8 are 8 high-accuracy thermocouples with 0.5 mm diameter, while T9-T14 are 1-mm-diameter. The vertical distance between any two thermocouples is 5 cm, where the first thermocouple T1 is 2 cm above the surface of the liquid fuel in pan. The vertical distance between each other for T9-T14 is 10 cm. T1-T8 are used to capture the temperature of main flame region, while T9-T14 are used to capture the temperature in the plume. Heat flux is measured by a radiometer, which is placed 60cm vertically from the pan surface and 48cm horizontally from the center of the pan. Mass loss rate is measured through high accurate electronic scale placed beneath the pan but separated by thermal resistance plasterboard. Chamber pressure and fire video were recorded along with other parameters. The data acquisition frequency for thermocouple and radiometer are 1 Hz.

The initial air temperature in the altitude chamber is 20 ℃ and the relative humidity is 50%. Each test was repeated three times to ensure a good data repeatability.

Fig 1: The altitude chamber and its pressure control system

Fig 2: The experiment setup in the chamber

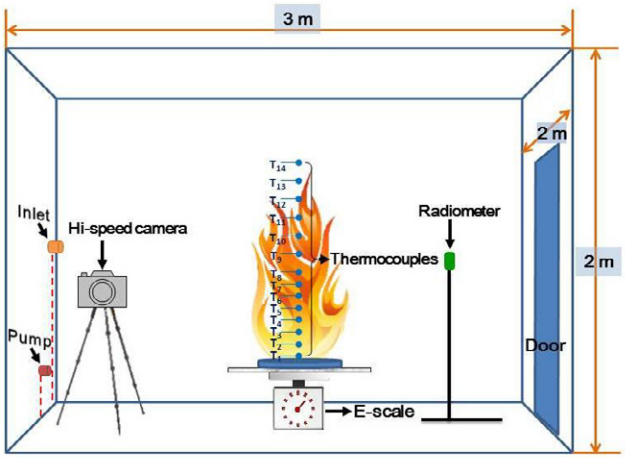

Fig 3: Experiment configuration

Table 1: Summary of fire tests in the low-pressure chamber

Fuel	Pan size	Dynamic Pressure	Measurement
n-heptane (C_7H_{16})	2-cm Height × **6**-cm Diameter (28 g fuel)	101.3→30 KPa (no air supply)	Axial temperature
Industrial purity ≥ 99%			
Density: 679.5 kg/m^3		101.3→30 KPa (+15 Nm^3/h)	Mass burning rate
Boiling point: 98-99 °C			Radiative heat flux
Auto-ignition temperature: 223.0 °C	2-cm Height × **10**-cm Diameter (80 g fuel)	101.3→30 KPa (+20 Nm^3/h)	Video record
Explosive limits: 1.05–6.7%			Chamber pressure
Specific heat: 224.64 JK^{-1}mol			

3. Results and discussions

3.1. Pressure descent rate

Fig 4 shows the average pressure descent rates for the two sizes of pool fires under different air supplying rates. In each test, the chamber pressure drops form 101.3 KPa to 34 KPa. The pressure is averaged over the 3 repeating tests for each combination case of pool fire sizes and air supplying rates. The air supplying rate is the main factor affecting the pressure descent rate, thus the data with the same supplying rate were plotted together, as in Fig. 4 (a), (b) and (c). It is shown that the average pressure descent rates of 10-cm-diameter pool fires are slightly lower than those of 6-cm-diameter pool fires, which can be attributed to that the larger pool fires release more heat during burning to expand the gas and increase the chamber pressure. The pressure curves were fitted by the exponential function to obtain the general curve trends. The average pressure descent rate without air supplying can be described as an exponential fitted curve of *101.3exp (-0.0016239×t)* with *t* time. Similarly, the average pressure descent rate with air supplying rate 15 Nm^3/h is described as *101.3exp (-0.0012516×t)*, and for the cases with air supplying rate of 20 Nm^3/h it is *101.3exp (-0.0011633×t)*. The descent rate of chamber pressure decreases as the increase of air supplying rate, which agrees with the expectation.

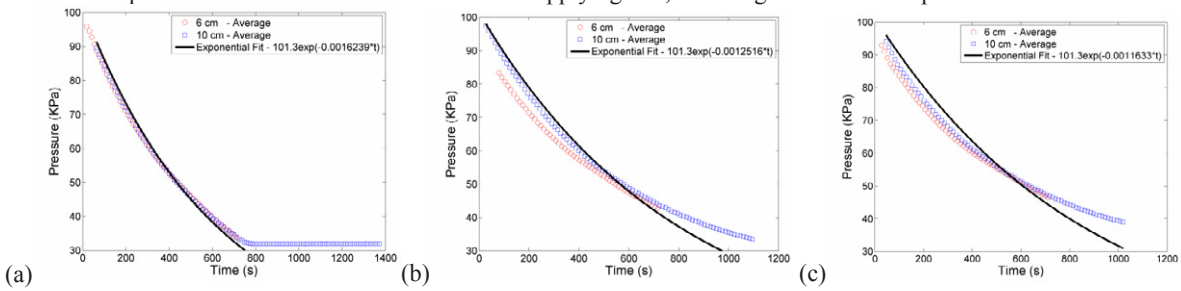

Fig 4: Chamber pressure vs. time for the air supplying rate of (a) 0 Nm3/h, (b) 15 Nm3/h and (c) 20 Nm3/h

3.2. Flame shape

Fig. 5 shows the flame shape under different pressures. When the pressure drops dynamically, the flame transmitted from turbulent to laminar, characterizing by the smoothing of corrugations on the flame envelop. As the flame transmitting from turbulent to laminar, the flame base turns from luminous amber to blue, which is because the reducing of soot volume fraction under low pressure [9, 10]. Before the fire extinguishment, the flame appeared as polyhedral shape and swirled in the pan until extinguishment. The laminar pattern is especially obvious and the blue region takes a large part in the flame when extinguishing. The appearance of polyhedral flame is because the large difference of heat and matter diffusion around the flame [11, 12]. The air entrainment significantly decreases when the flame transmitting from turbulent to laminar under low pressure, but the burning rate of fuel maintains on the same level, thus the axial gas velocity becomes larger than the radial

gas velocity. Then the flashover in the flame core drastically expands volume of the hot combustion products, consequently forming polyhedral flame [13]. The most striking characteristic of polyhedral flame is self-swirl, which is to maintain the stability of burning flame [13]. Previous observed polyhedral flames are mainly in laminar premixed flames [14], while the polyhedral flames in laminar diffusion flames are not frequently reported. The critical conditions for the appearance of polyhedral flame are strict, e.g. the axial fuel velocity should neither be smaller than radial entrainment velocity, nor too larger to produce a jet flame. The swirling speed of the polyhedral flame is mainly determined by the fuel exit velocity.

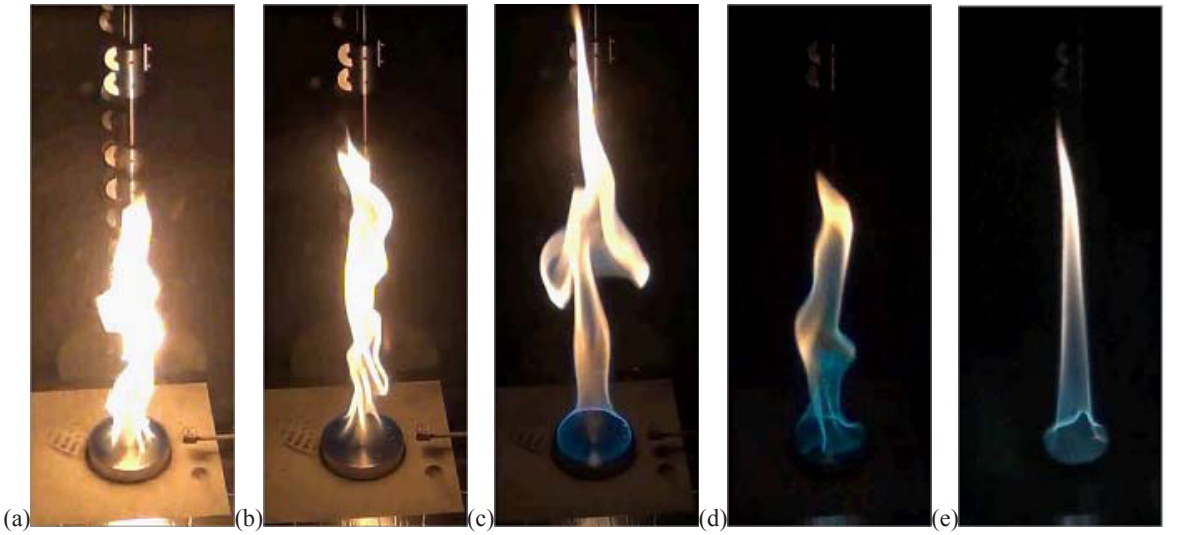

Fig 5: N-Heptane10 cm pool fire flame shape change vs. pressure change, (a) 89 KPa, (b) 68 KPa, (c) 35 KPa, (d) 32 KPa, (e) 32 KPa (at extinguishment)

3.3. Mass burning rate

Fig 6 shows the burning rates versus pressure for the 6cm and 10cm pool fires under different air supplying rates, i.e. 0, 15 and 20 Nm^3/h. The burning rates were average over the 3 repeating tests to show the general trends. During the burning process, the temperature of the liquid fuel was increased gradually by the convective and radiative heat feedback from the flame and the surrounding (e.g. chamber walls and hot smoke layer) until boiling if the burning time is long enough, which makes the burning rate increase gradually [15]. Theoretically, the radiative and convective heat feedback decreases under low pressure, which will decrease the burning rate without considering the preheating effect [16]. The curve trends shown in Fig. 6 are the combined effect of depressurization and heating up of the fuel. The burning rate is steady approximately in the first half period after ignition, in which stage as the chamber pressure drops the burning rate decreases slightly. In the second half period, while the fuel temperature is increasing, the burning rate increases drastically. When the fuel burns out at the end, the burning rate decreases again until the fire is extinct. In contrast to the cases with air supplying, the same quantity of fuel burns longer under the condition of no air supplying, because the pressure decreases faster without air supplying and the burning rate is phenomenally lower at low pressure. Generally, the burning rate increases with the increasing of pan size (until a ceiling value) [17, 18], because of the increased heat feedback (mainly radiative component). Comparing to the larger 10-cm-diameter pool fires, the small amount of fuel in the 6 cm pan is preheated to boiling faster; therefore the burning rates of 6-cm-diameter pool fires increase more dramatically.

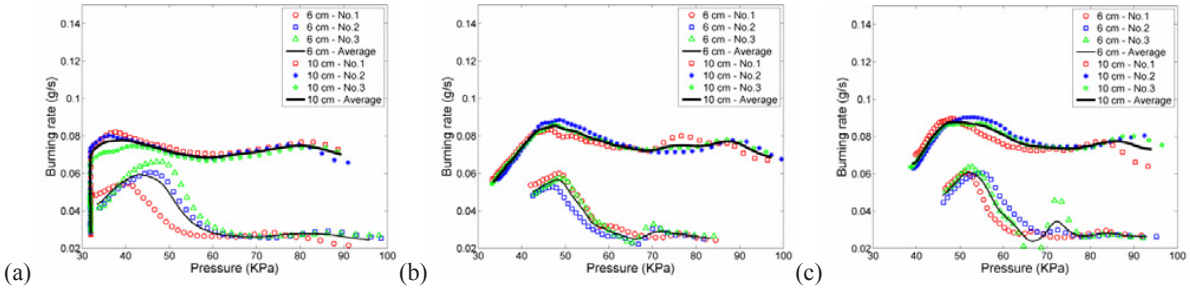

Fig 6: Burning rate vs. pressure, (a) without air supplying, (b) air supply rate 15 Nm^3/h and (c) 20 Nm^3/h

3.4. Flame temperature

The temperature measurement for each thermocouple was averaged over the 3 repeating tests and plotted together in Fig. 7 to show the general trends of axial temperature. The repeatability of 3 tests for each case is reasonably good, especially for higher axial height where the temperature fluctuations are small. The temperature is affected by both the pressure and the fuel burning rate. Generally, the axial plume temperature decreases with the increasing of height, and increases with the decreasing of pressure for that the fuel/air increases. Besides, as the soot production decreases (denoted by the blue flames), the decrease of radiative heat loss also increases the flame temperature. As pressure drops, the flame height increases, which is equivalent to moving the relative position of thermocouples downward to the fuel side. Temperature drops for thermocouples at low height were observed during the depressurization, which can be attributed to the decreases of mass burning rate when pressure drops.

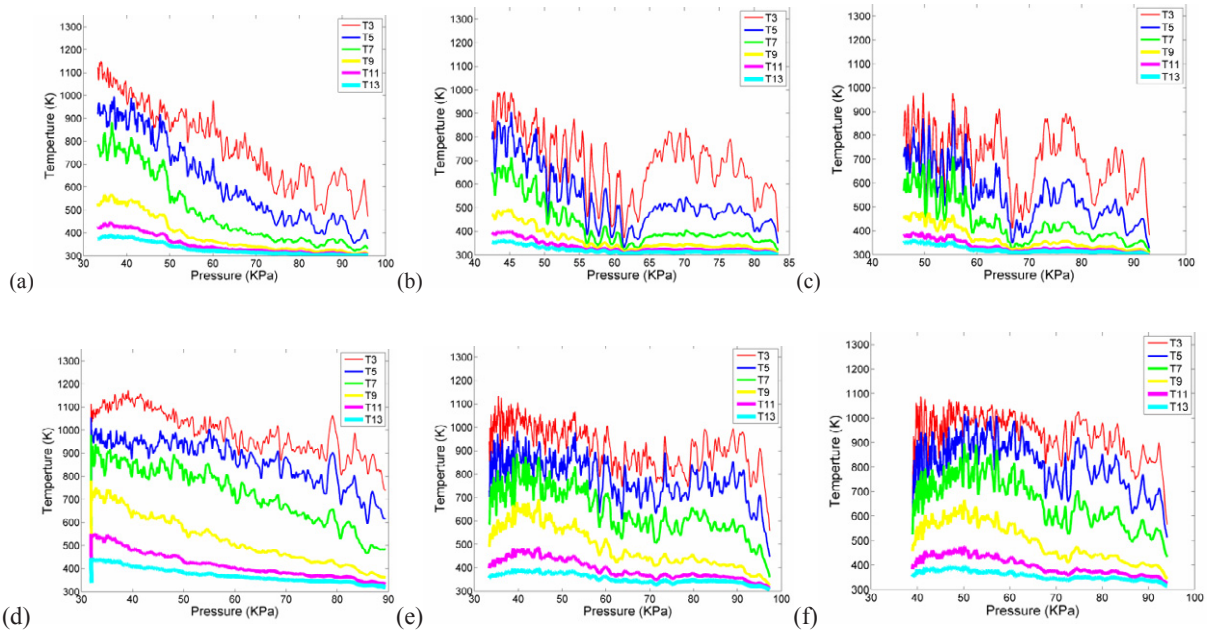

Fig 7: Average temperature vs. pressure, 10 cm pan: (a) no air supplying, (b) air supplying rate 15 Nm3/h, (c) 20 Nm3/h; 10 cm pan: (d) no air supplying, (e) air supplying rate 15 Nm3/h, (f) 20 Nm3/h

Besides pressure and mass burning rate, radiation fraction is an important factor in affecting the flame temperature [19]. Previous experiments show that the radiation efficiency has low dependence on pressure, due to counteracting effects of the decrease in flame surface area and the increase in soot formation [20],

$$X_r \sim P^{-0.1} \tag{1}$$

Then, the relationship of plume temperature, axial height and pressure can be written as [19, 21],

$$\frac{T_p - T_\infty}{T_\infty} = C_T \left(\frac{1 - X_r}{c_p T_\infty \sqrt{g}} \right)^{2/3} \left((Z + Z_0) \frac{\rho_\infty^{2/5}}{\dot{Q}^{2/5}} \right)^{-5/3} \sim \left((Z + Z_0) \frac{P^{2/5}}{\dot{Q}^{2/5}} \right)^{-5/3} \tag{2}$$

where $\dot{Q}$ is the total heat release rate, c_p is the thermal capacity, ρ_∞ and T_∞ is environment density and temperature respectively, g is the gravity. Virtual origin Z_0 is defined by Heskestad equation [21], which is a function of pan size D and $\dot{Q}$. Fig. 8 presents the linear fit of the plume temperature measurements by the thermocouple T3-T13 based on Eq. (2), where heat release rate is estimated by the burning rate and the heat of combustion of N-Heptane. Fig. 8 shows a good linear

relationship, which demonstrates that the axial plume temperature increases when the pressure decreases under the same burning rate.

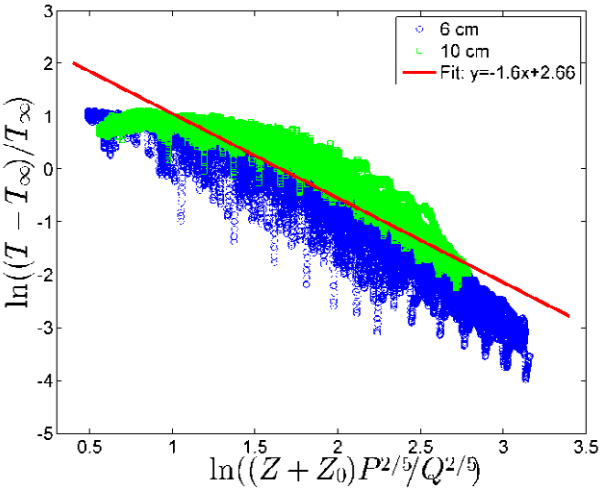

Fig 8: The relationship between dimensionless plume temperature and dimensionless axial height with pressure term

3.5. Radiative heat flux

Fig 9 presents the relationship of the radiation heat flux and the pressure of pool fire. Basically the radiation heat flux is the same as the trend of the burning rate. At the pressure drops, the flame height increases and the soot radiation decreases (denoted by the blue flames), all those factors affect the heat flux measured by the radiometer, which was fixed.

Because the radiative heat flux was measured in a far distance (horizontal distance comparable with the flame height) from the pool fires, the radiative heat flux can be considered to characterize the overall radiation output from the flame and the plume. The flame radiation output is a function of overall flame emissivity ε_f and overall flame temperature $T_{f,o}$ from the general equation [16],

$$\dot{Q}_r'' = \varepsilon_f \sigma T_{f,o}^4 = \left(1 - e^{-\alpha L_e}\right)\sigma T_{f,o}^4 \tag{3}$$

where σ is Stefan-Boltzmann constant. Eq. (3) shows that the flame emissivity is determined by the absorption coefficient α and the mean beam length L_e in the flame. Absorption coefficient consists of the gas compound α_g and the soot component α_c [22, 23] , where soot is the main radiation contributor [24]. The soot volume fraction f_v is related to pressure by

$$f_v \sim P^2 \tag{4}$$

Therefore, it has

$$\alpha = \alpha_g + \alpha_s \approx \alpha_s \sim f_v \sim P^2 \tag{5}$$

For the moderately-sooting fuel N-Heptane [9], the examined pool fires can be assumed as optically thin, i.e. αL_e is small, especially under low pressure where soot production is even lower. Then Eq. (3) can be approximated by,

$$\dot{Q}_r'' = \left(1 - e^{-\alpha L_e}\right)\sigma T_{f,o}^4 \approx \alpha L_e \cdot \sigma T_f^4 \sim P^2 T_{f,o}^4 \tag{6}$$

Then further from Eq. (2) and Eq. (6), the overall flame temperature is scaled with pressure and fire load,

$$T_f \sim \left(P/\dot{Q}\right)^{-2/3} \sim \left(\dot{Q}_r''/P^2\right)^{1/4} \tag{7}$$

Fig. 10 shows the plotting of Eq. (7), where fit of radiative heat flux data validates the linear relationship very well. From Eq. (7), it is shown that the radiative heat flux is correlated with the pressure to the power of -2/3 for the same mass burning rate. But since the mass burning rate decreases under low pressure, the radiation output reduces yet.

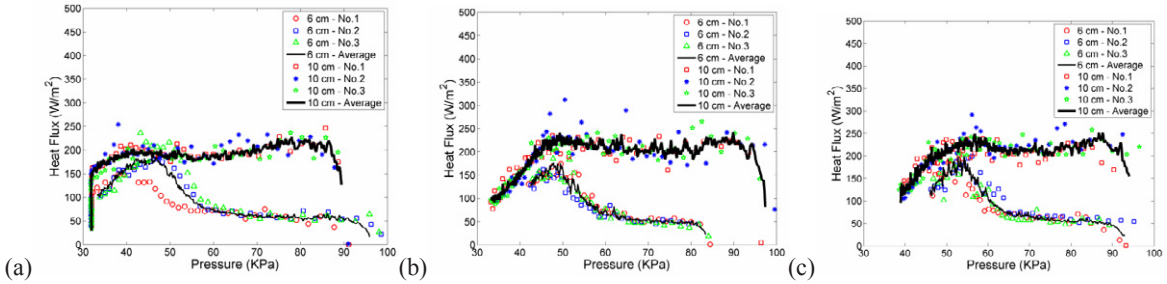

Fig. 9: Radiation heat flux vs. pressure, (a) no air supplying, (b) air supplying rate 15 Nm3/h and (c) 20 Nm3/h

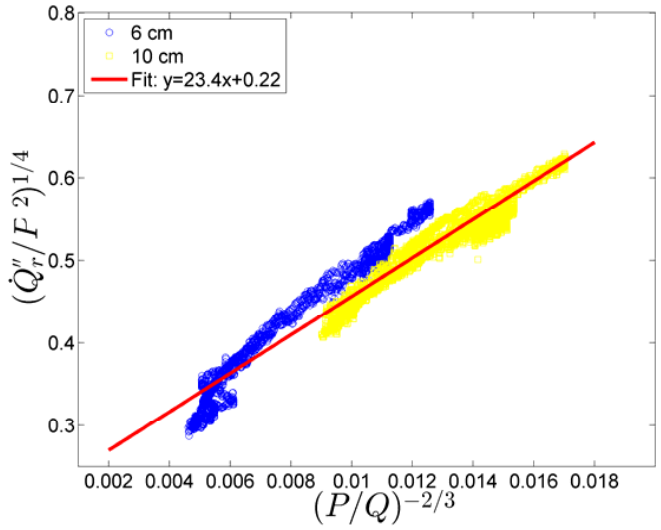

Fig. 10: The linear relationship of radiative heat flux vs. pressure and fire load

4. Conclusions

This studies tests the fire behaviors of two sizes of N-Heptane pool fires under dynamic pressure in an altitude chamber. From the analysis of the experimental data, the main concluded can be draw as follows,

- As the chamber pressure drops, some special phenomena on flame pattern were observed: the flame transmitted from turbulent to laminar, characterized by the smoothing of corrugations on the flame envelope; the flame turned blue from the base due to the decreasing of soot volume fraction; below a certain pressure, a polyhedral laminar diffusion appeared and swirled in the pan until extinguishment.
- The real mass burning rate is affected by the combination effect of pressure and fuel temperature. As pressure drops, the heat feedback from the flame to the fuel surfaces decreases thus the mass burning rate decreases. On the other hand, the preheating of liquid fuel by continuous heat feedback increases the fuel temperature till boiling, which will increase the burning rate. Both the two different trends were observed for the burning of pool fires during depressurization.
- The dimensionless plume temperature is correlated with the pressure to the power of -2/3, which indicates that the plume temperature rises as pressure drops for the same burning rate.
- Assuming an optical thin flame for the moderately-sooting N-Heptane fueled flames, the radiative heat flux is correlated with the pressure to the power of -2/3 for the same burning rate. But since the mass burning rate decreases under low pressure, the radiation output yet reduces.

In this study, the correlations of fire behaviors with pressure were analyzed based on some assumptions, because the burning rate is not only affected by pressure but also by fuel temperature. However, it would be better to directly observe the fire behaviors under dynamic pressure by excluding influence of the fuel temperature. In the future tests, cooling

apparatus should be designed to maintain the liquid fuel temperature at a fixed point, then the relationship between fire behaviors and pressure can be directly observed and validated.

Acknowledgements

This work was partially supported by the National Basic Research Program of China (973 Program No：2012CB719705), National Natural Science Foundation of China (Grant No.91024032, 70833003) and China Postdoctoral Science Foundation (No: 023261011).

References

[1] Wieser, D., Jauch, P., Willi, U., 1997. The influence of high altitude on fire detector test fires. Fire Safety Journal 29, p. 195.
[2] Li, Z., He, Y., Zhang, H., Wang, J., 2009. Combustion characteristics of n-heptane and wood crib fires at different altitudes. Proceedings of the Combustion Institute 32, p. 2481.
[3] Hu, X., He, Y., Li, Z., Wang, J., 2011. Combustion characteristics of n-heptane at high altitudes. Proceedings of the Combustion Institute 33, p. 2607.
[4] Fang, J., Yu, C., Qiao, L., Zhang, Y., Wang, J., 2008. The influence of low atmospheric pressure on carbon monoxide of n-heptane pool fires. Journal of Hazardous Materials 154, p. 476.
[5] De Ris, J., Kanury, A.M., Yuen, M.C., 1973. Pressure modeling of fires. Proceedings of the Combustion Institute 14, p. 1033.
[6] Alpert, R.L., 1977. Pressure modeling of fires controlled by radiation. Proceedings of the Combustion Institute 16, p. 1489.
[7] Hill, R., 2009. 2009 FAA fire safety highlights. Federal Aviation Administration, Washington, DC.
[8] Fang, J., Tu, R., Guan, J., Wang, J., Zhang, Y., 2011. Influence of low air pressure on combustion characteristics and flame pulsation frequency of pool fires. Fuel 90, p. 2760.
[9] Yao, W., Zhang, J., Nadjai, A., Beji, T., Delichatsios, M.A., 2011. A global soot model developed for fires: Validation in laminar flames and application in turbulent pool fires. Fire Safety Journal 46, p. 371.
[10].Yao, W., Zhang, J., Nadjai, A., Beji, T., Delichatsios, M., 2012. Development and validation of a global soot model in turbulent jet flames. Combustion Science and Technology 184, p. 717.
[11].Ming-Yan, G., Guang, C., Shi-Shuang, X., 2002. Analysis of the polyhedral flame of premixed laminar combustion. Journal of Engineering Thermophysics 23, p. 523.
[12].Buckmaster, J., 1984. Polyhedral fames - an exercise in bimodal bifurcation analysis. SIAM Journal on Applied Mathematics 44, p. 40.
[13].Ming-yan, G., Guang, C., Li-zheng, L., Tian-hu, M., 2002. Experimental research on the polyhedral flame of butane premixed laminar combustion. Journal of Combustion Science and Technology 8, p. 525.
[14].Smith, F.A., Pickering, S.F., 1928. Bunsen Flames of Unusual Structure. Industrial and Engineering Chemistry 20, p. 1012.
[15].Yao, W., Yin, J., Hu, X., Wang, J., Zhang, H., 2012. Numerical modeling of liquid n-heptane pool fires based on heat feedback equilibrium, The 9th Asia-Oceania Symposium on Fire Science and Technology, Hefei, China.
[16].Koseki, H., Mulholland, G.W., 1991. Effect of diameter on the burning of crude oil pool fires. Fire Technology 27, p. 54.
[17].Hall, A.R., 1972. Pool burning: a review. Rocket propulsion establishment, Westcott.
[18].Quintiere, J.G., 2006. Fire plumes, Fundamentals of fire phenomena. John Wiley & Sons, pp. 297-336.
[19].Most, J., Mandin, P., Chen, J., Joulain, P., Durox, D., Fernande-Pello, A.C., 1996. Influence of gravity and pressure on pool fire-type diffusion flames. Proceedings of the Combustion Institute 26, p. 1311.
[20].Heskestad, G., 1983. Virtual origins of fire plumes. Fire Safety Journal 5, p. 109.
[21].Lautenberger, C.W., John L. De Ris, N., Dembsey, A., Barnett, J.R., Baum, H.R., 2005. A simplified model for soot formation and oxidation in CFD simulation of non-premixed hydrocarbon flames. Fire Safety Journal 40, p. 141.
[22].Lautenberger, C.W., 2002. CFD simulation of soot formation and flame radiation. Worcester Polytechnic Institute.
[23].De Ris, J.L., Wu, P.K., Heskestad, G., 2000. Radiation fire modeling. Proceedings of the Combustion Institute 28, p. 2751.